REDUCED SUSCEPTIBILITY OF DEFORMATION DUE TO VIBRATIONAL AND GRAVITATIONAL EFFECTS ON A FOCUS VARIABLE ADAPTIVE LENS

by

VICTORIYA RELINA
B.S. Florida Atlantic University, USA, 2007

A thesis submitted in partial fulfillment of the requirements
for the degree of Master of Science
in the College of Optics and Photonics
at the University of Central Florida
Orlando, Florida

Spring Term
2013

Major Professor: Shin-Tson Wu

ABSTRACT

Orthodox optical devices, such as lenses, mirrors, and prisms, are composed of solid-state materials, which although well studied and implemented ubiquitously are severely limited in their adaptable properties. An arguably new field of adaptive optics has emerged to further expand photonic manipulation competences of optical components. Fluid-based adaptive optical components were introduced as early as 1968 [1]; such components have the ability to change the shape of their interface surface, thus allowing for a variable curvature profile.

The method of manipulation varies greatly, as does the range of surface deformations. A solid-state optical component is affected by system vibration variation only (difference in vibration from one component to the other due to damping effect). By comparison, two large limiting factors of a fluid-based adaptive optical component are the effect of local vibrations on the surface of the device and gravitational effect (when the optical axis of a lens is positioned parallel to gravitational pull). Such a gravitational effect has been mitigated by the invention of the mechanical electrowetting lens [2], which uses density matching of two liquids that make up an adaptive lens. However, this configuration creates an extra limiting factor of density matching two optically clear fluids with a desirable transmission spectrum. This method can also become bulky when a large aperture is needed.

In this thesis, two adaptive lens systems are explored. Principles of operation, performance, limitations, as well as future improvements are studied and theorized.

The first lens uses an optically clear elastomer as the substrate of an adaptive lens and a primitive mechanical manipulation to turn a plano–plano lens into a plano–convex lens. The second lens is composed of an optically clear gel rather than a fluid. Both methods exhibit excellent optical properties regardless of the orientation about the gravitational pull and significantly limit local vibration affects simply by the physical nature of the chosen materials.

This thesis is dedicated to my family.

ACKNOWLEDGMENTS

This thesis would not be possible without the great support and patience of Prof. Shin-Tson Wu and his brilliant group. Never in my life have I met a group of people so knowledgeable and devoted to their work.

There were only two factors that made me choose Dr. Wu's group for a thesis study, my interest in adaptive optics and the well-known and remarkable reputation of Dr. Wu, who has the patience of a saint and an uncanny ability to inspire his pupils to produce award-winning results at a pace most companies couldn't even dream of. Dr. Wu, you are an inspiration to us all.

An extra special "thank you" has to be mentioned to Su (Tracy) Xu and Yuan (Esther) Chen. I can't help but think that I have wasted many hours of your time, yet neither one of you ever made me feel unwelcome. I would be plagiarizing if I did not mention that most of my work is based on the work that Tracy trail brazed before me.

I am also very thankful to all of my committee members. Thank you for taking time out of your busy schedules. It is truly appreciated.

A special "thank you" has to be mentioned to Dr. Joel Olson from Florida Institute of Technology. Thank you for being kind to a graduate student. I hope our paths will cross again.

Finally, my acknowledgment statement could not be complete without thanking my amazing (one-of-a-kind) family, friends, DRS Technologies, and numerous acquaintances for being always supportive of my dubious schemes, having agreed to help me against their best judgments. And last but not least, many "thank-yous" to my forever patient, understanding, loving husband. I promise to spend a little more time at home and a little less at work

TABLE OF CONTENTS

LIST OF FIGURES

LIST OF TABLES

LIST OF NOMENCLATURE

AR	Anti-reflection
BFL	Back focal length
CA	Clear Aperture
EDS	Energy Dispersive X-ray Spectroscopy
EL	Elastomeric lens
GL	Gel lens
IR	Infrared
LC	Liquid crystal
lp	Line pairs
NIR	Near infrared
PDMS	Polydimethylsiloxane, brand name Sylgard® 184
SEM	Scanning Electron Microscopy
USAF	U.S. Air Force

CHAPTER 1. INTRODUCTION TO FLUID-BASED ADAPTIVE OPTICS

1.1 Background

Unlike conventional, solid-state, optical components, an adaptive optical component (lens, as an example) has an uncanny ability to vary its focal length without the use of additional lenses or zooming schemes. Wavefront correcting optical components, adjustable iris, and optical switching are other forms of adaptive optics; however, this document will solely concentrate on focal length variability.

Focal length of a standalone thin (1) and thick (2) lens is dependent on the index of refraction n of the substrate material, lens thickness d and the curvature of two surfaces R_1 and R_2 that make up a lens. This relationship is described by well-known lens equations:

Thin lens equation $$1/f \approx (n-1)[\frac{1}{R_1} - \frac{1}{R_2}] \quad (1)$$

Thick lens equation $$\frac{1}{f} \approx (n-1)\left[\frac{1}{R_1} - \frac{1}{R_2} + \frac{(n-1)d}{nR_1R_2}\right] \quad (2)$$

Although materials such as liquid crystal (LC) can manipulate the index of refraction, the manipulation of the radius of the curvature is of interest in this document.

Several tunable polymer lens designs have been explored [2], [3], [4], [5], [6]; however, most of these designs rely on polydimethylsiloxane (PDMS) as a flexible membrane encapsulating a fluid or use combination fluids to create a curvature. A limited amount of work has been devoted to researching the choice of using solid-state polymer [7] to make the lens substrate.

1.2 Curvature Manipulation

Adaptive lenses have many different curvature manipulation mechanisms and configurations. Because the adaptive lenses described in this document are mechanically actuated, it is worth looking into works performed before [8], [9], [10].

Unlike mechanically actuated manipulation mechanisms, electronically tunable lenses have the added benefit of no moving parts; however, time dependency begins to take affect [11], [12], [13]. Issues of hysteresis and high driving voltage must be considered when picking an electrically driven mechanism.

Although tunable index of refraction materials [14] and devices [15] exist, the most prominent being LC [16], all such materials and devises have limitations. This document will only focus on mechanically manipulated devices because of their ease of accessibility and low cost.

1.3 Motivation

The more common fluid-based adaptive lenses are comprised of a flexible membrane that makes up either both or just a single surface of a lens, a liquid (typically water) that makes up the bulk "substrate" of a lens, and a curvature manipulation mechanism. Such a focus-variable lens was demonstrated by Ren and Wu [17] and is depicted in Figure 1.1.

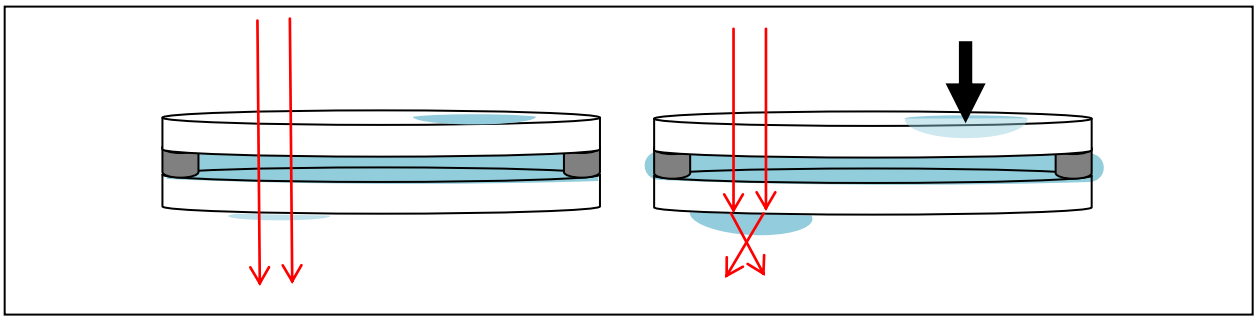

Figure 1.1: Light passing through a clear housing and flat membrane (left); pressure being applied to the top flexible rubber, causing the flexible membrane on the bottom to inflate and converge light (right)

1.4 Deficiencies of Adaptive Lenses

Currently, some adaptive lenses suffer from an unintentional deformation due to environmental effects. If the center of gravity of the lens does not match the optical axis, gravitational pull could distort the lens. For example, if the lens in Figure 1.1 were to be turned upright (turned 90º), the aberration due to gravitational pull would be severe enough to cause loss of image quality, specifically, asymmetry.

Another environmental effect, that could unintentionally degrade an adaptive lens performance, is vibration. If a vibration source (such as loud music) were to be placed near this lens, ripples would form on the membrane surface.

If lens, composed of water, were to be placed inside an electronic device and membrane were to suffer a catastrophic failure due to, as an example, sever environmental exposure well beyond established system limits, water could liberate inside the device. This could cause damage to components nearby. Such deficiencies prevent adaptive lenses from becoming more commonly used in complex and reliability-dependent devices.

1.5 Improvements to Adaptive Lenses

The absorption spectrum of water limits the operability of the lens to the visible region. Other liquid solvents, such as acetone and hexane improve the range but introduce the issue of toxicity. New “substrate-less” fluidic, yet still adaptable, materials are explored in this document in an attempt to compensate for limitation of solvents.

The mechanism of manipulation as well as lens performance have been improved by many researchers. Mechanisms driven by pressure [2], [4], [5], [6] [10], hydrogels [18], [19], electrowetting [20], [21], [22] have been reported and characterized. Although vibrational and gravitational effects have been minimized by the introduction of electromechanical wetting [21]; however, none of those improvements are enough to make a durable adaptive lens ready for the less forgiving (non-ideal lab) setting.

1.6 Summary

To summarize, four main concerns are explored in this document:

- Gravitational effect
- Local vibrational effect
- Index of refraction strength limitations
- Absorption spectra

CHAPTER 2. LIQUID VIBRATIONS AND GRAVITATIONAL PULL

Many mathematical formulas describe membrane [23] and liquid vibrations [24]. In all cases, density of perturbed substance is taken into consideration. Density is inversely proportional to the wave field densities of volume [25] force and vertical displacement [26]. Not surprisingly, higher density lowers the amplitude and therefore the displacement of waves on a surface of a membrane and liquid. This means using higher density materials reduces surface waves (ripples) of a liquid-based lens.

Although using a solid material will eliminate this problem completely, focus variability will become significantly diminished or non-existent. Vibration propagation on a flexible surface does not only occur on the density of the chosen material, but also on the bond stiffness of which the material is composed.

Vibrations are damped by turning mechanical energy into thermal energy (which is then dissipated). Elastomer's ability turning mechanical energy into thermal energy is directly related to the long chain molecules coiling and uncoiling. As per its definition, elastomer's molecules must be very long (chain-molecules) and be able to rotate around the bond (links) of neighboring molecular chains and must have small intermolecular attraction [27]. It is this weak force between molecules that allows for molecules to stretch apart when a force is applied. This is why elastomers make great vibration dampers and are a good choice as substrate material for an adaptive lens, especially when vibrations are a concern.

To further study the effect of vibrations as a degradation factor on adaptive lenses, a solid (BK7) lens, water-filled lens, Gel Lens (GL), and Elastomer Lens (EL) were subjected to

vibrations with the profile described in Figure 2.1 and Figure 2.2. The vibration source was attached to a variable lens holder, which was capable of mounting all four lens types.

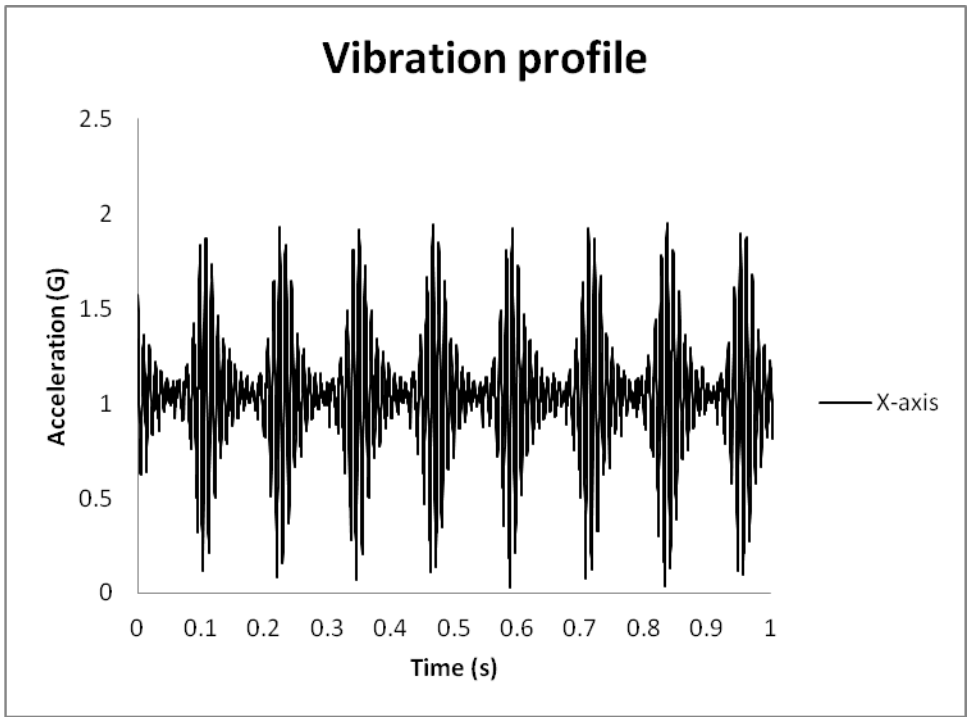

Figure 2.1: Test vibration profile-acceleration vs. time

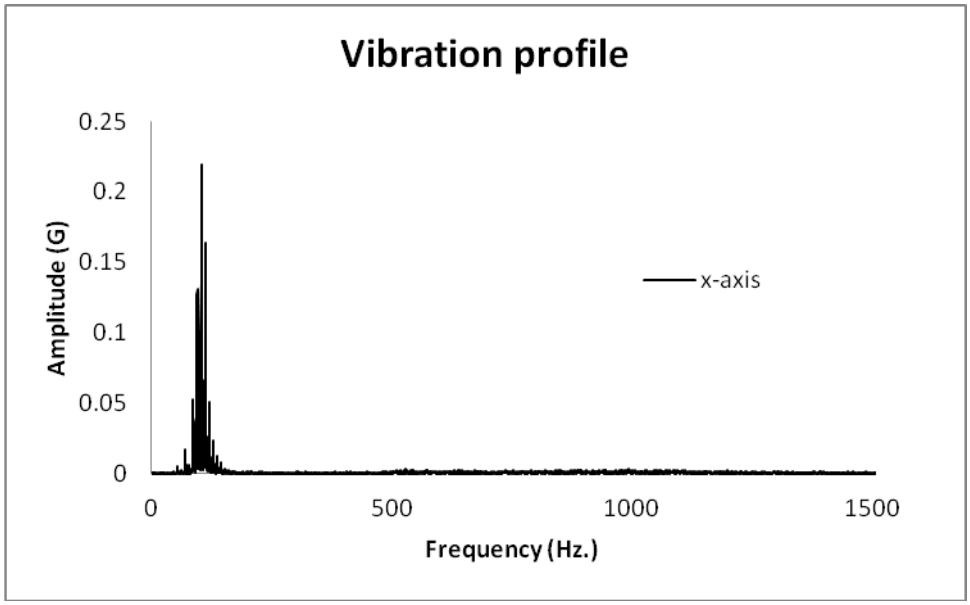

Figure 2.2: Test vibration profile: amplitude vs. frequency

The image quality of all subjected lenses was evaluated using a Michelson interferometer. Snapshots of each interferogram can be found in Figure 2.3. All appear to be defocused. EL is suffering from some astigmatism and spherical aberration. The water-filled lens and GL suffer from spherical aberration and tilt [28].

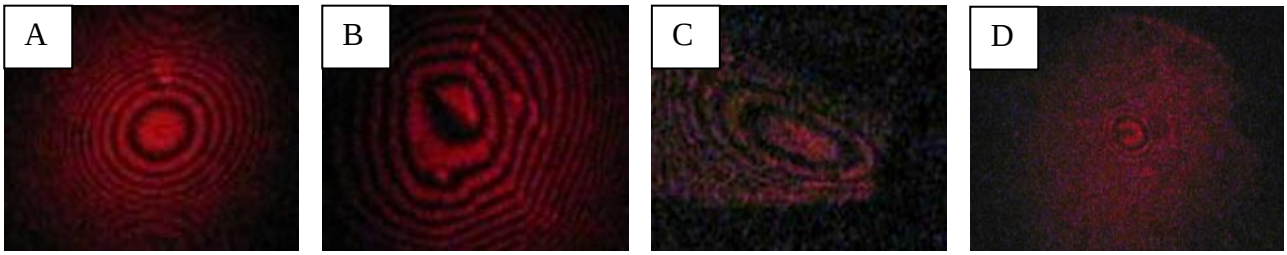

Figure 2.3:Test interferograms: A) glass lens, B) EL, C) GL, D) water-filled lens; all subjected to vibration profile described in Figure 2.1 and Figure 2.2

The EL asymmetric wavefront error is likely caused by the square glass slide that provided the entrance aperture backing. Using a circular glass that matches the diameter of EL would eliminated such distortion.

Table 2.1: Fringe Shift Evaluation of GL, EL, Glass, and Water-filled Lens Under Vibration

	GL	EL	Glass lens	Water-filled Lens
Number of fringes	2	0	1	2

The number of fringes that moved from the center of each inteferogram, tabulated in Table 2.1, was counted by extracting frames from a video file of each lens, performance, and overlaying images. EL was able to absorb the most, and the water-filled lens and GL performed the worst. This could be caused by the type of housing chosen for GL and the water-filled lens.

Another degradation factor of fluid-based adaptive lenses is gravitational pull. A fluid lens deforms when turned upright so that the optical axis, of a side mounted lens, runs perpendicular to gravitational pull similar to the way a cantilever beam deforms due to gravitational pull as shown in Figure 2.4.

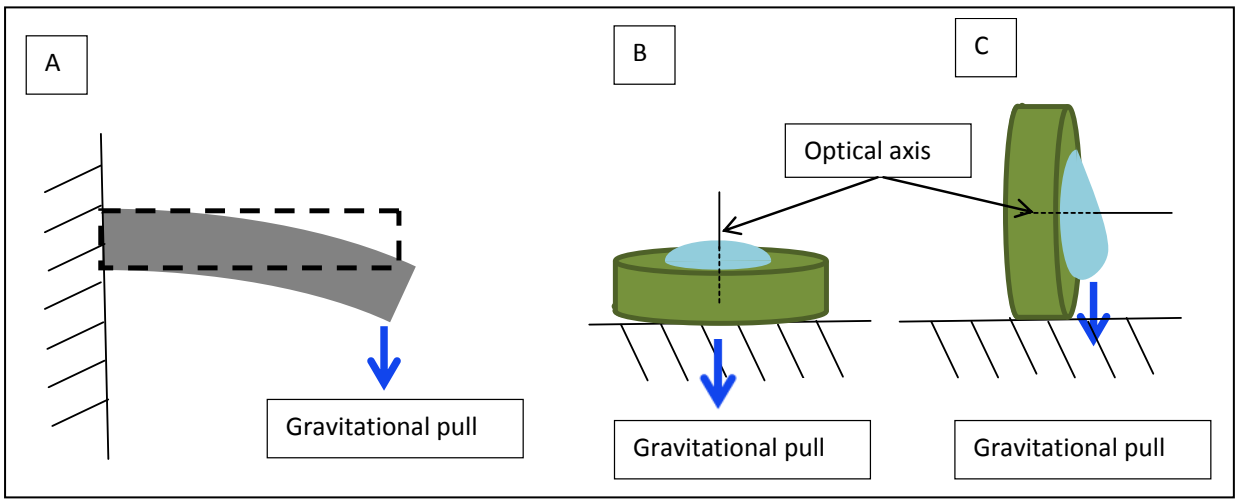

Figure 2.4: A) Cantilever beam under gravitational pull, B) fluid lens with optical axis parallel to gravitational pull, C) fluid lens with optical axis perpendicular to gravitational pull.

If a cantilever beam is affixed at one side, maximum deflection caused by a force of the end of the cantilever is described by a well-known equation (3):

$$\delta = \frac{FL^3}{3EI} \tag{3}$$

where δ is the deflection of the beam, F is the force applied to the beam, L is the length of the beam and/or location of the force inflection point, E is Young's modulus, and I is the moment of inertia. Because the gravitational pull is uniformly distributed along the beam, the point of inflection must be moved to the center of the beam by dividing L by a factor of 2.

Obviously, deformation of a liquid lens will not follow the same formula as a straight and a rigid beam, but the physical principles are the same. Deflection of a lens apex depends on Young's modulus and geometry; however, there is no Young's modulus for water.

The following equations are from Hooke's law and Lame's elastic coefficients μ and γ as constraints [29]:

$$K = \frac{3\gamma + 2\mu}{3} \tag{4}$$

$$\gamma = \frac{\sigma E}{(1+\sigma)(1-2\sigma)} \tag{5}$$

$$\mu = \gamma\left(\frac{1}{\sigma} - 1\right) \tag{6}$$

where E is Young's modulus, σ is Poisson's ratio, and K is the bulk modulus. A simplified relationship between Young's modulus and Bulk modulus (which is known for liquid and solid phases) using Poison's ratio is described below:

$$K = \frac{E(\sigma+2)}{3(1+\sigma)(1-2\sigma)} \tag{7}$$

Rewriting in terms of Bulk modulus

$$E = \frac{K[3(1+\sigma)(1-2\sigma)]}{\sigma+2} \tag{8}$$

Poisson's ratio for liquids (zero rigidity) is σ~0.5 [30]. This reduces the equation above to $E = 0$. In an attempt to get an appreciation of the deflection of water encapsulated by an elastic membrane, a more indirect comparison of bulk modulus is explored. Bulk modulus of water is on the order of 2 GPa. Comparing this to 40 GPa bulk modulus of glass gives a factor of 20 (Table 2.2). The true factor is significantly higher because of Poison's ratio but is impossible to calculate using the formulas above. If a $\lim_{\sigma \to .5}(E)$ is taken, elastic modulus goes to infinity.

Table 2.2: Approximate Physical Properties for Glass, Steel, Water, and Rubber[a] [31], [32], [33]

Material	Young's Modulus ($10^9 N/m^2$)	Bulk modulus ($10^9 N/m^2$)	Poisson's ratio (unitless)
Glass	~70	~40	~2
Structural Steel	200	160	.3
Water		2.15	.5
Rubber	~0.5	2.15	.35

[a] Selected for comparison purposes only; not to be used as absolute values.

Because Young's modulus for elastomers is readily available, obtaining deflection is possible. Rubber (an elastomer) has Young's modulus on the order of 0.05×10^9 N/mm^2 (this number varies depending on the exact rubber formulation). Young's modulus of glass is on the order of 65×10^9 N/m^2. Even though the difference is on the order of 1000, the deflection is insignificant because a typical lens thickness in the direction of deflection is on the order of several mm, but even this small of a distance becomes a deformation concern when the bulk material of a lens is in liquid state.

A simulation of an elastomer plano-plano lens, 7mm in diameter and 3mm thickness was modeled using Pro-Engineer software. Poisson's ratio assumed to be 0.4 and Young's modulus of $0.5 \cdot 10^9 N/m^2$. Lens was affixed by one flat surface and gravitational pull applied perpendicular to the optical axis, approximately as depicted in Figure 2.4. Results are displayed in Figure 2.5 below.

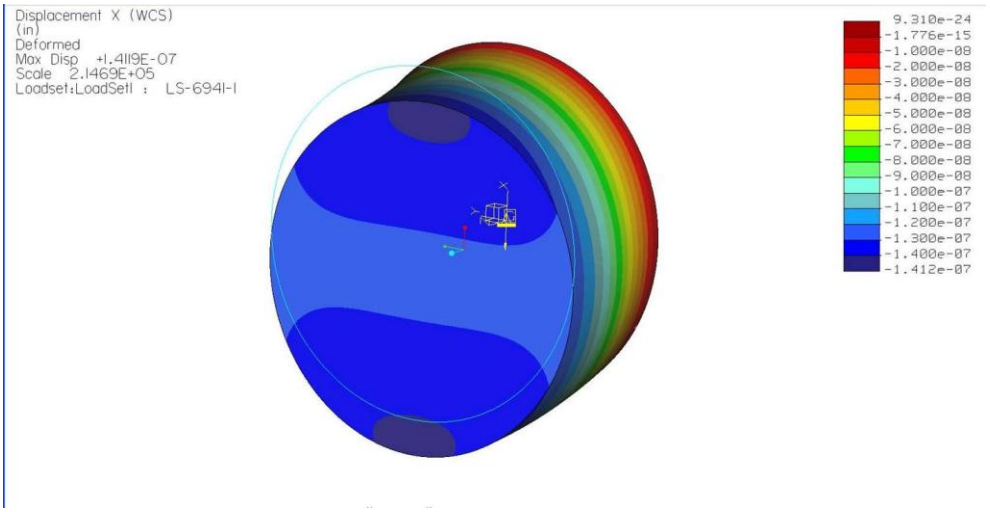

Figure 2.5: A simulation of an elastomer plano-plano lens, 7mm in diameter and 3mm thickness.

Maximum displacement (deformation) in downward direction was simulated to be 3.6μm. When a plano side is replaced with a perfect hemisphere, as depicted in Figure 2.6, the maximum displacement (deformation) has decreased to 2.8μm.

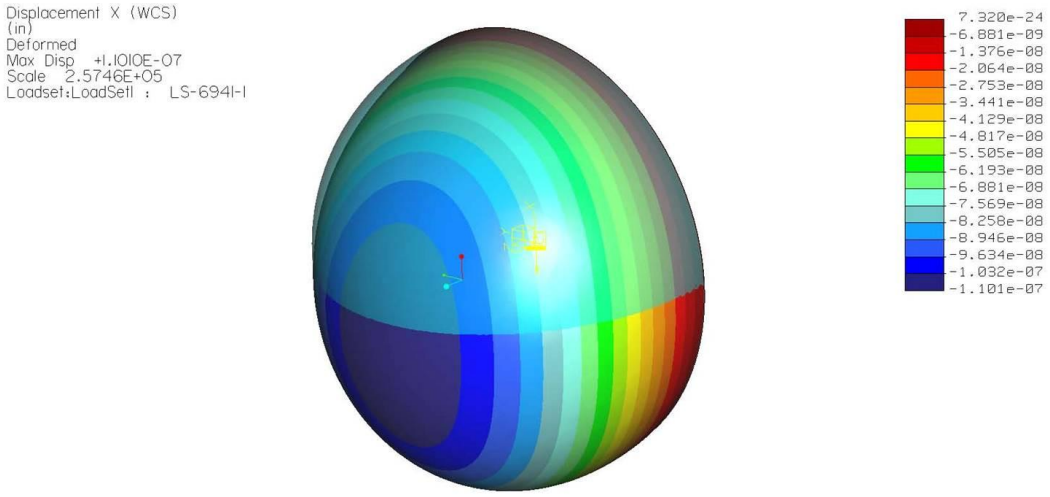

Figure 2.6: A simulation of an elastomer hemi-sphere lens.

Mathematical modeling of liquid-filled tunable lenses with PDMS membrane has been performed by Qingda Yang [34], where Young's modulus and the pre-strain can be found by

measuring peak deflection versus pressure. Inversely, if Young's modulus and pre-strain are known, the radius of curvature and the conic constant (resulting from mounting imperfections/high points) can be accurately predicted.

CHAPTER 3. ADAPTIVE ELASTOMER LENS

This chapter describes an elastomer lens made out of NuSil's LS-6941 optically clear silicone elastomer, refractive index 1.41. The low Shore hardness A of 30 and 100% elongation before failure allow for significant focal length manipulation, while allowing for complete self-containment if a catastrophic failure were to take place.

3.1 Preparing the Lens

The elastomeric lens (EL) was prepared by trapping uncured elastomer material between two plano surfaces with a 6 mm spacer (chosen to fit off-the-shelf housing parts) in between and allowed to cure at ambient temperature. The spacer dimensions (specifically perpendicularity) were closely controlled so wedge would not be introduced. To prevent wavefront error, the contacting surface of the aperture, where the EL would protrude, had to be very smooth and uniform. A vacuum was pulled around the uncured EL lens to ensure all air bubbles were eliminated. The cure temperature was kept ambient to prevent unnecessary internal stress. The two plano surfaces had very low surface energy, which allowed for an easy removal of the EL. Once the elastomer was cured, EL was carefully removed.

3.2 EL Manipulation

Figure 3.1 shows the EL manipulation mechanism. This particular mechanism was chosen for its simplicity, low cost, and accessibility. Other more sophisticated mechanisms can be used to make the focus variability a more automated process.

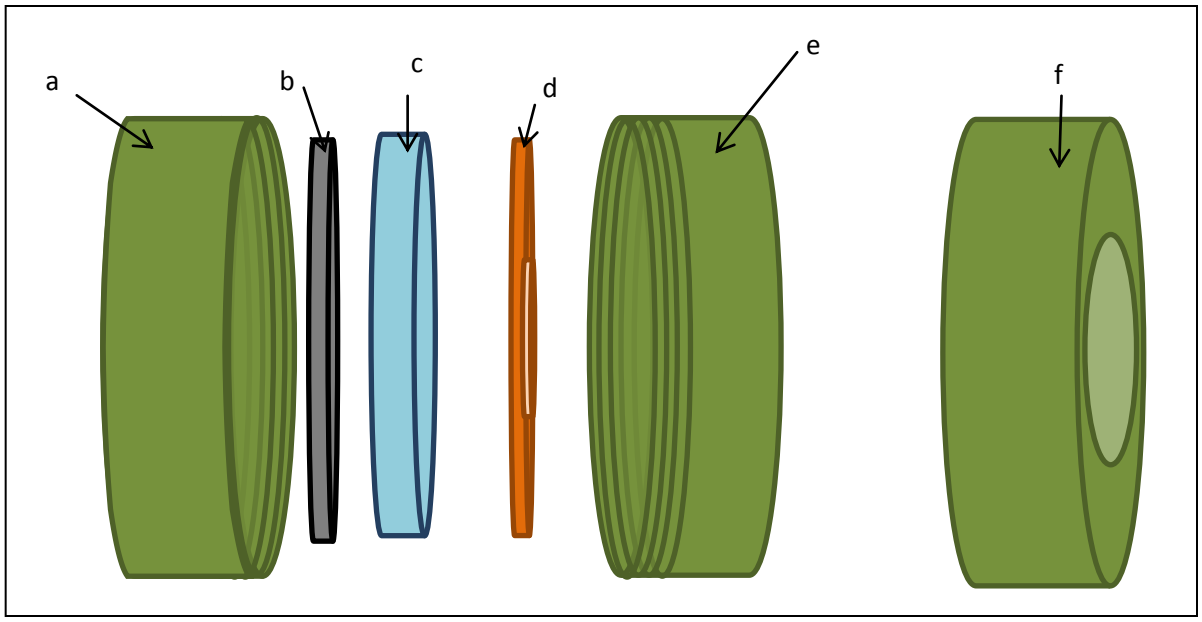

Figure 3.1: EL manipulation mechanism: a and e are the housing compartments, b is a glass slide, c is the EL, d is the aperture, and f is the backside with entrance and exit pupil of the two housing components, respectively.

Housing compartments were made to thread into one another, while trapping the remaining EL components in between. As the volume inside the housing became more restricted, the EL began to protrude through the aperture, and the lens became a plano–convex lens with curvature varying with housing threading (Figure 3.2). The pitch of the threads and the diameter of the elastomer dictate the minimum change in focal length (Δf). Using a smaller thread pitch size and a larger diameter/area of elastomer further decreases Δf.

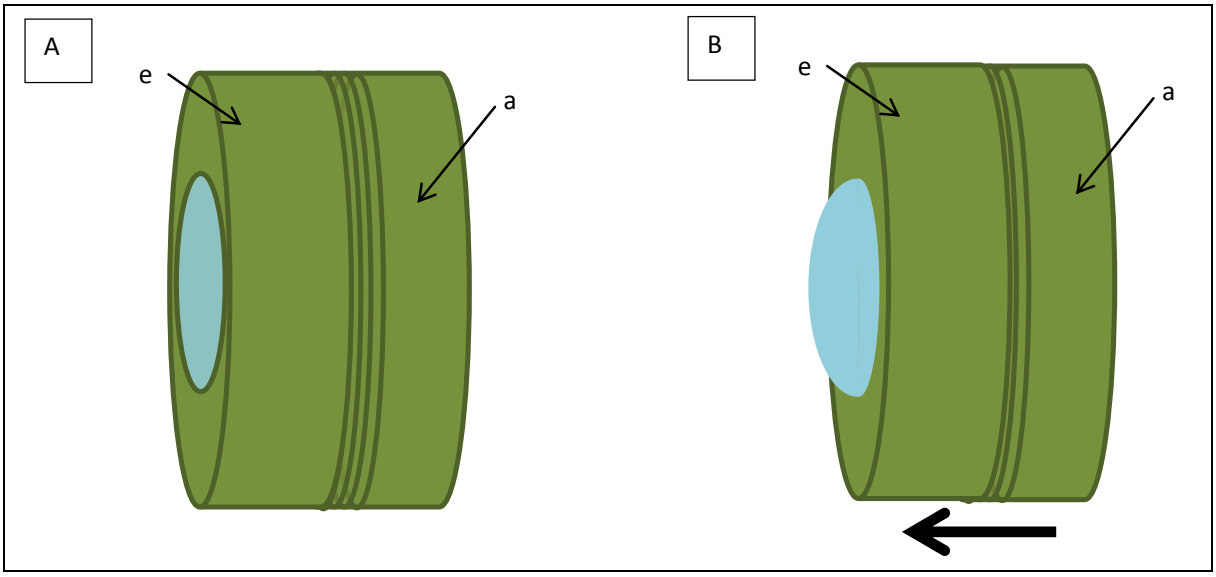

Figure 3.2: EL phases. A is the EL in its relaxed (plano–plano) phase, and B is the EL threaded (plano–convex) phase.

The focal length, at a maximum threaded phase, measured 44 mm. The power of this variable lens can be further increased by replacing the glass slide with a second aperture, which causes the lens to become a convex–convex lens as the housing was threaded further.

When the EL was turned under a 90º angle, no difference in performance, because of gravitational pull, was noted.

3.3 Calculating Deflection

Deflection due to gravitational pull was calculated using a readily available formula [32] (refer to CHAPTER 2). The formula for moment of inertia *I* for a circular beam, radius r, with a circular cross section Eq. (9) is

$$I = \frac{\pi r^4}{4} \tag{9}$$

If a glass lens made of BK7 with density of 2.51 g/cm^3, thickness of 7 mm, and radius of 3 mm, were to be affixed as described by a cantilever beam in Figure 2.4A, moment of inertia *I* would equate to 6.36 x 10^{-11}m^4. Applying the deflection formula and Young's modulus factors

for glass from CHAPTER 2 deflection, for the above described scenario, for glass lens equated to 13.5 nm. If the same calculation were repeated for rubber, 71.9 nm of deflection would be derived. Although a rubber material lens (and therefore the EL described in this document) would obviously deform more than a glass lens would, a rubber lens would still exhibit significantly less deflection than a liquid-filled lens would.

3.4 Measuring Index of Refraction

The index of refraction was measured using a Variable Angle Spectroscopic Ellipsometry (VASE) technique. VASE measures amplitude ψ and phase difference Δ of ellipsometric angles. To find the refractive index, the ratio of these values were used to fit a curve from where Cauchy's formula coefficients can be extrapolated [35].

Figure 3.3 shows the VASE curve for a sample of cured LS-6941 elastomer Cauchy's coefficients measured at A=1.396, B= 0.00395, and C=8.6861x10^{-5} within .2 nm accuracy.

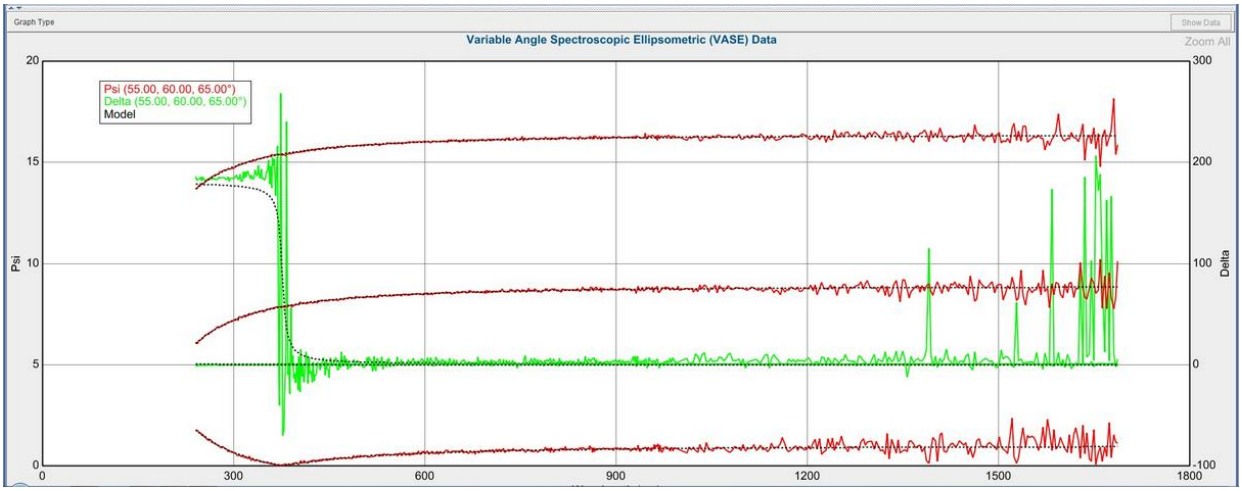

Figure 3.3: VASE Ψ and Δ curves, used to fit Cauchy's coefficients for the dispersion formula, of LS-6941.

Using Cauchy's formula [36] as shown in Eq. (10) below, where *n* is the index of refraction and λ is wavelength, the index of refraction was calculated.

$$n = A + \frac{B}{\lambda^2} + \frac{C}{\lambda^4} \tag{10}$$

Results are shown in Figure 3.4.

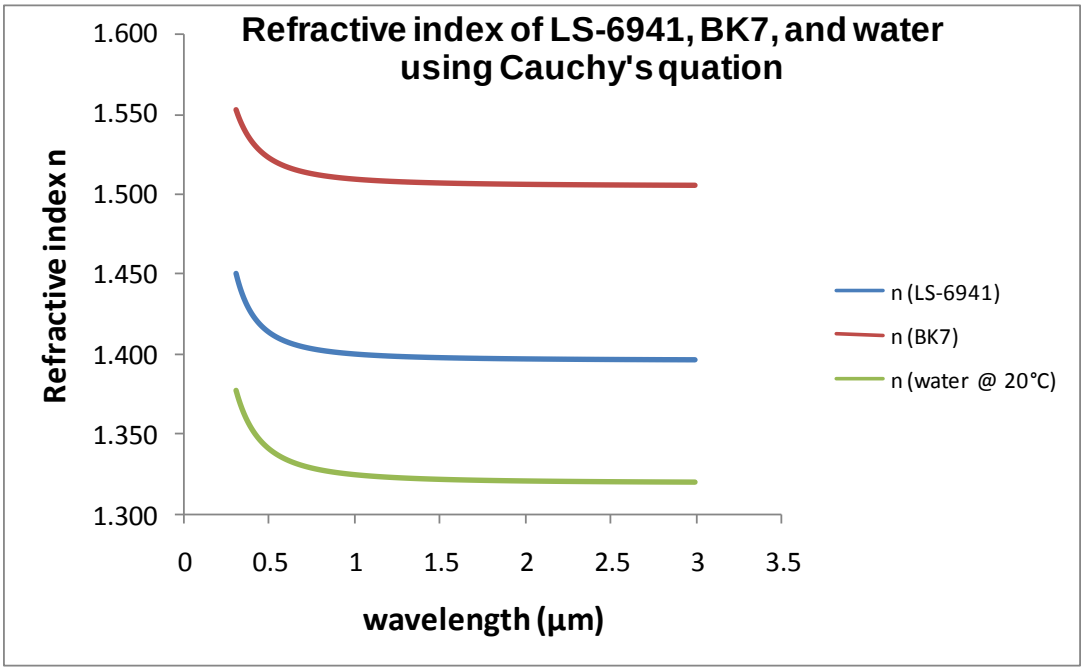

Figure 3.4: Refractive index of LS-6942, BK7, and water plotted using Cauchy's equation.

Although LS-6941 has a lower index of refraction than BK7, its index of refraction is higher than that of water. An elastomer with a higher index of refraction can be chosen to further improve the focal-length range of an EL by increasing optical lens power.

3.5 Measuring Transmission

The transmission of 6mm EL with a 1 mm glass slide was measured using spectrophotometer from 300 to 3000 nm. Results are shown in Figure 3.5. Transmission of LS-6941 is excellent through the entire visible range and almost throughout the entire (near-infrared) NIR region, including 75% transmission between 850 and 1550 nm, commonly used wavelengths for free space optical communication [37]. At 1550 nm, communication strength

signal is eye safe. These wavelengths are also preferred because of a lack of water absorption bands [38,39] both in liquid and gas phase.

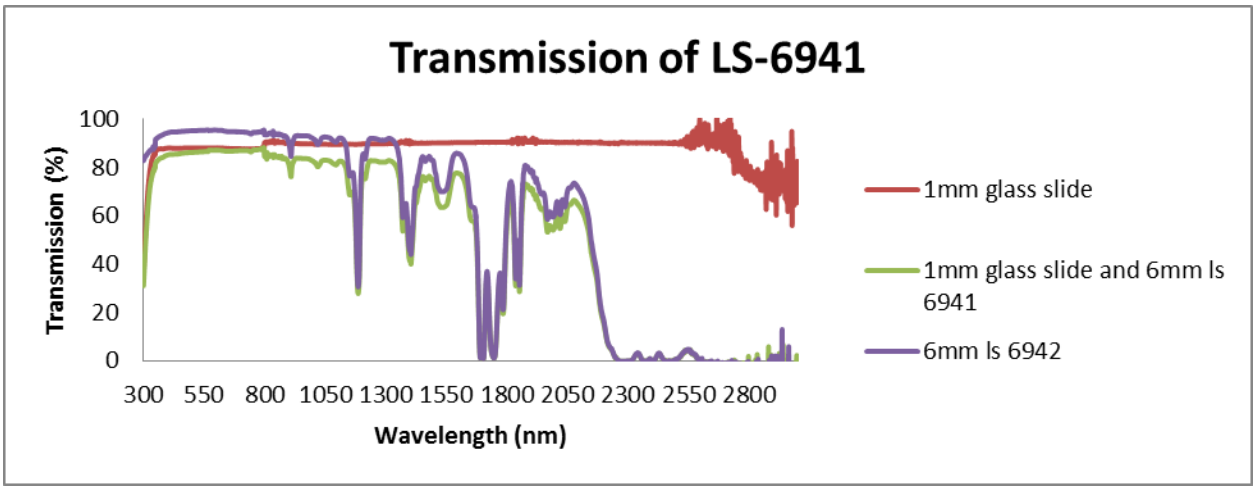

Figure 3.5: Transmission spectrum of a 6mm EL lens with a 1 mm glass slide.

The spectrum can be varied by choosing a different elastomer with favorable physical properties. Many different optically clear elastomers are commercially available. Shore hardness A of 30 is on the lower limit of optically clear elastomers, but the elongation of 100 is very low (per ASTM1566-11, elongation of 100 is the absolute minimum to be qualified as an elastomer).

SEM/EDS analysis of LS-6941 (Figure 3.6) revealed presence of silicon, carbon, and oxygen. SEM/EDS is unable to detect hydrogen (among a few other elements); however, the presence of hydrogen is very likely because of the common hydrogen vibration band, which can be clearly seen as a drop in transmittance in the NIR region [40].

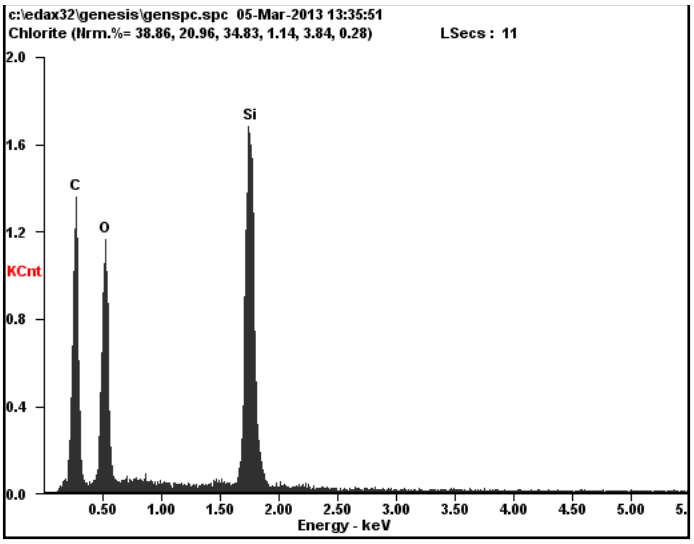

Figure 3.6: SEM/EDS analysis of LS-6941.

Absorption band between 1100 and 1225 nm was due to the second overtone (molecular anharmonic vibrations) of C-H stretching. The second absorption band, around 1400 nm, was caused by a combination stretch of C-H. The large drop between 1650 and 1800 nm was attributed to the first overtone of C-H stretching [41]. The strong absorption beyond 2000nm for an organic compound is attributed to 1) closely overlapped absorption bands of fundamental and overtone vibration bands, and 2) a fairly thick film (6 mm). Infrared absorption bands for silicone compounds begin showing starting at 2700 nm and proceed into the far infrared region [41], [42]. A complete infrared spectrum must be run to determine absorption band with certainty.

3.6 Measuring Focal Length

Focal length of the EL lens was approximated by placing the maximum threaded (plano–convex state) EL in front of collimated and expanded He–Ne laser beam (Figure 3.7) and the

minimum spot size location was traced (see Figure 3.8). The back focal length (BFL) (and in this case, same as the focal length) was found to be 44 mm. Clear aperture (CA) of EL was 9.5 mm.

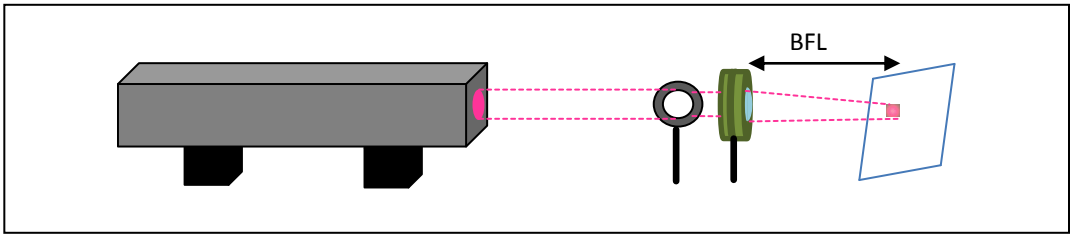

Figure 3.7: Experimental setup used to determine maximum focal length of EL.

Using the thick lens formula and index of refraction data, the convex radius was derived to be –17.91mm.

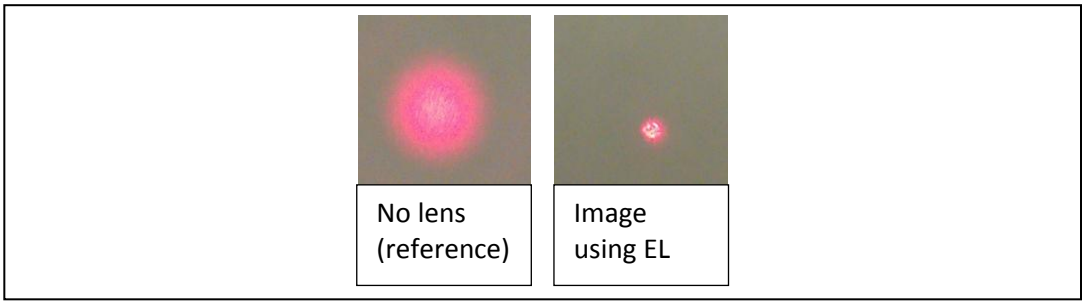

Figure 3.8: Reference image (left) and image taken with maximum threaded EL (right).

3.7 Evaluating Gravitation Effects

Gravitation effects were evaluated by imaging through the EL lens in both vertical and horizontal orientations. As expected, little to no discernible effect (See Figure 3.9) was noted because cured LS-6941 elastomer is a solid-state material.

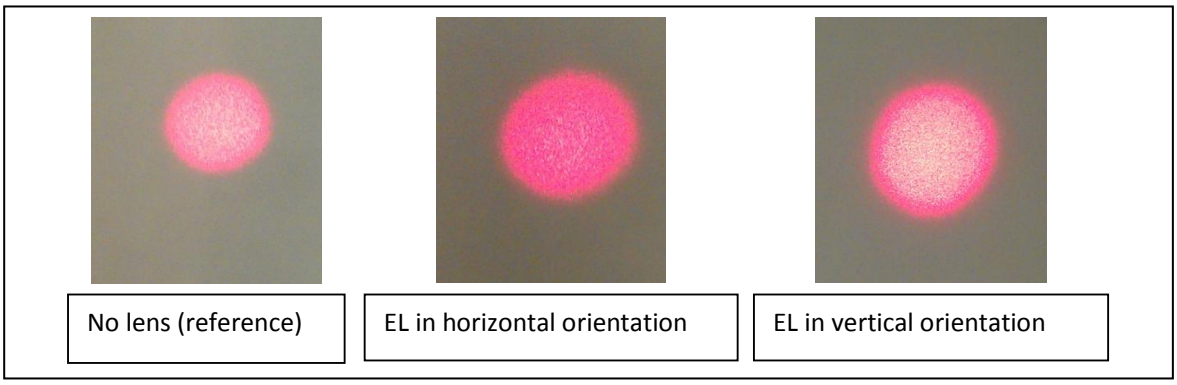

Figure 3.9: Evaluation of gravitational pull on EL in vertical or horizontal orientation.

3.8 Determining the Resolution

To determine the resolution of the EL, a 1951 U.S. Air Force (USAF) resolution target was placed directly under the EL and imaged via a microscope. The exact magnification and resolution setting and capability of the used microscope were not known, so results were approximate. In Figure 3.10, a reference resolution target, imaged through the microscope, was able to resolve Group 3 Element 6, which equated to 14.3 line pairs (lp) per mm.

When an unthreaded (flat) EL was placed on top of the target, resolution decreased to Group 3, Element 3, which was 10.10 lp per mm. This suggests that EL was either not exactly plano–plano and/or caused scattering. Both deficiencies could be easily corrected with improved manufacturing techniques.

When EL was threaded, resolution increased slightly back to Group 3, Element 6, which was 14.30 lp per mm. At the threaded state, strong barrel distortion was observed. Barrel distortion could be easily corrected via image processing software.

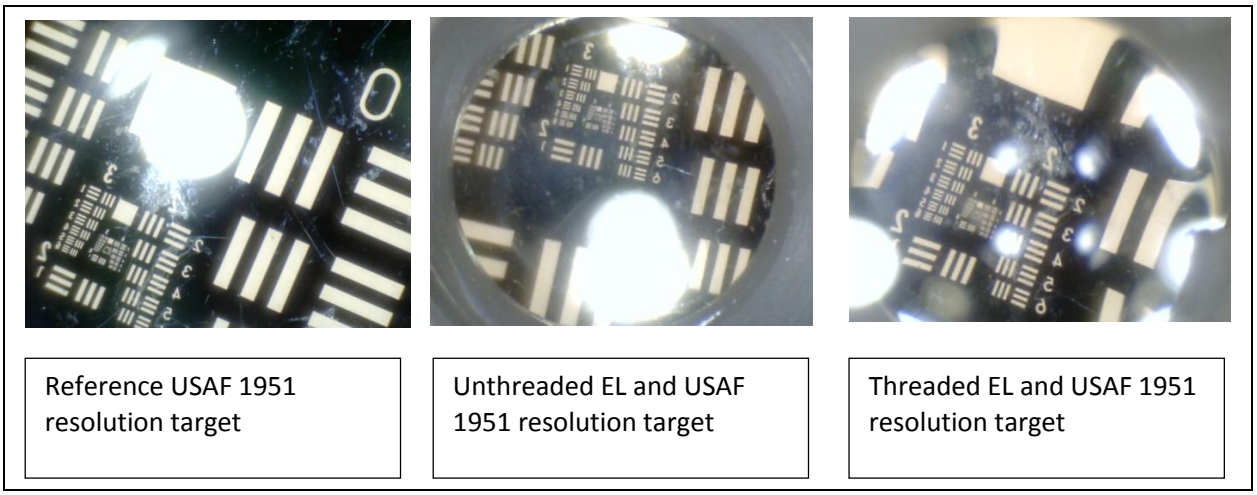

Figure 3.10: Resolution evaluation of El using a USAF 1951 resolution target.

Magnification range of an object is shown in the images in Figure 3.11. As with the resolution target, barrel distortion can be seen.

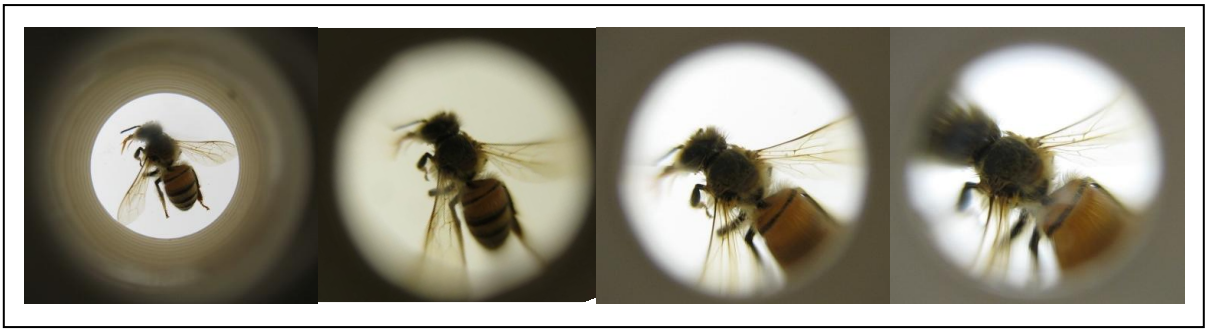

Figure 3.11: Magnification progression of EL on an image.

3.9 Summary

This chapter described the demonstration and characterization of an elastomer lens. This simple lens was easy to manufacture with low-cost supplies. A simple mechanical manipulation allowed the curvature of the lens to be changed from plano–plano to plano–convex. The focal length was varied from infinity to 44 mm. Transmission of EL was possible from visible to NIR range.

The mechanical manipulation method was chosen for its simplicity and availability (off-the-shelf components were used). This simple manipulation method allows for compatibility with a large variety of optical systems. Because LS-6941 elastomer is in a solid state, this setup would be attractive for any application that must withstand vibrational shock and have the ability to be operated in any orientation.

CHAPTER 4. ADAPTIVE GEL LENS

The major limiting factor of ELs is the focal length range. If the EL were squeezed too far, the lens would pass its deformation limit, suffer catastrophic failure, and not be able to return to the initial state. A new alternative of an optically clear gel "substrate" is presented in this chapter.

4.1 AL-1246 Gel

AngstormLink's AL-1246 [43] thixotropic optically clear gel was used as a "substrate" for a novel gel-based adaptive lens. AL-1246 is commercially available and is used for index matching to silica (1.46) when a low modulus gap medium is needed for photonic elements. This gel is also used for telecommunications coupling of silica Kber splices.

AL-1246 is non-migrating, which means when a small amount of dispensed gel is placed on an area, the gel does not spread out or deform for an extend period of time. This property makes this gel a very simple and attractive alternative to liquids, which are typically used for adaptive lenses. Unlike any other liquid state "substrate," including a higher viscosity oil, deformation due to gravitational pull is negligible. Additionally, thixotropic gel performs much better in presence of vibrations when compared to liquid because this gel is much closer to a solid state than a liquid state.

4.2 Cell Design

To test AL-1246 thixotropic gel, a new cell design was created. This cell was enclosed completely to contain the gel. Figure 4.1 shows the basic gel lens (GL).

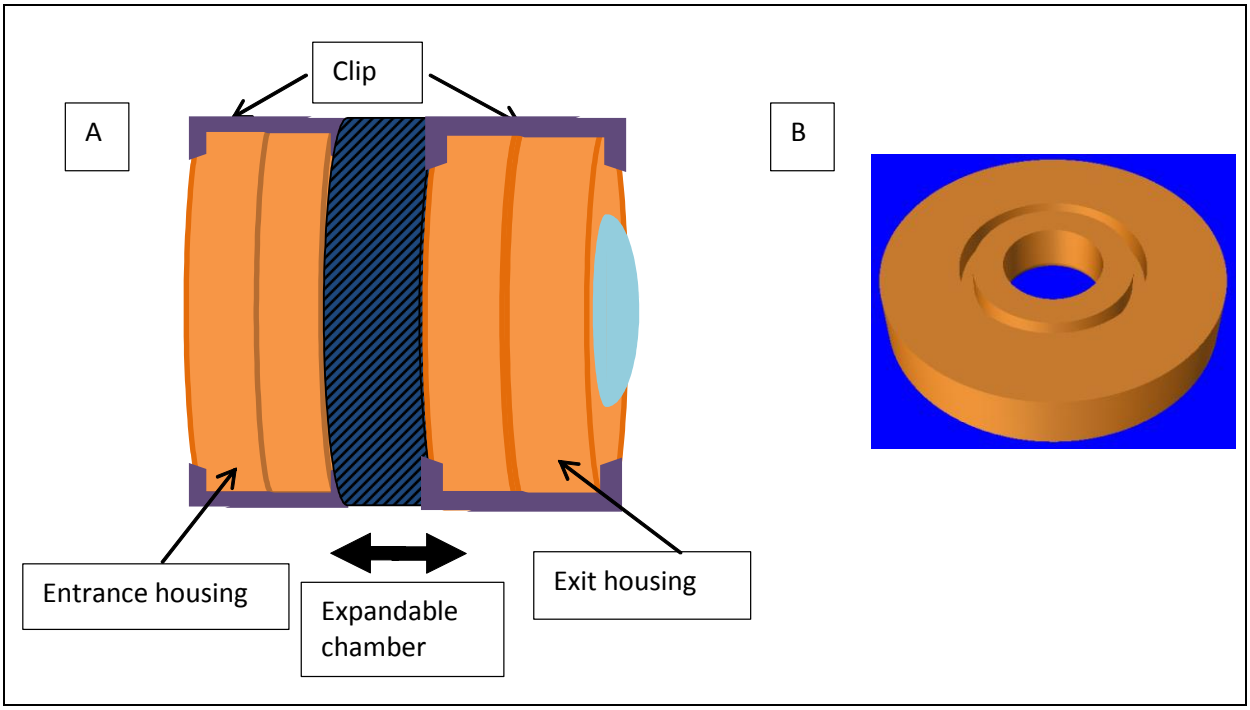

Figure 4.1: Basic gel lens. A) GL cell made from 4 sub-housings, B) sub-housing

The sub-housing was designed with a flat surface on one side and a groove on the other. A PDMS membrane was sandwiched between two flat sides of the sub-housing and held together using two clips making up the exit housing.

The same steps described above were repeated but instead of a PDMS membrane, a glass slide was used, which made up the entrance housing. An expandable chamber made out of a pliable plastic was used to connect both housings. The initial state of the GL cell required for the expandable chamber to be partially expanded. Thixotropic gel was introduced prior to sealing the glass containing the sub cell.

4.3 Manipulating the Gel Lens

At the initial state of the GL cell, both sides of the GL were plano. If the expandable chamber was extended, the GL became plano–concave. If the chamber was collapsed, GL became plano–convex. Theoretically, a glass slide could be replaced with another flexible membrane, making GL vary from a convex–convex to concave–concave lens; however, a plano–plano state proved to be challenging because of the nature of thixotropic gel. The thickness of the collapsible grooves and the diameter of the chamber directly affected Δf (minimum focal length difference). Increasing both, the chamber diameter of groove thickness will further decrease Δf.

Images in Figure 4.2 were made using a GL and water-filled lenses. An expanded He–Ne laser was imaged through the lens. Images were taken with lenses in vertical and horizontal positions. Similarly, one image was taken with GL in horizontal position and another in vertical. Some asymmetry differences can be clearly seen in Figure 4.2; however, when the gel was replaced by water and the same cell was used, the difference between the orientations of the water-filled lenses was stark.

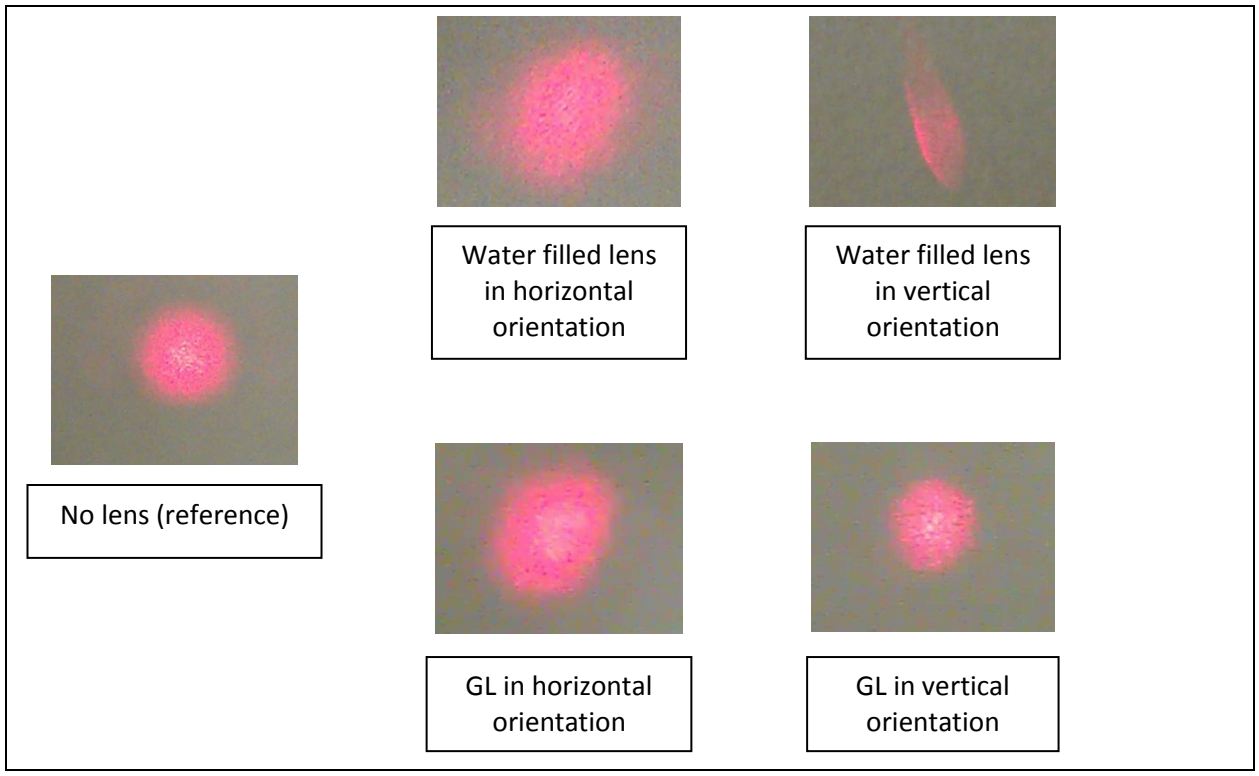

Figure 4.2: Images taken using a water-filled adaptive lens and GL in vertical and horizontal orientations.

4.4 Measuring Transmission

The transmission of an AL-1246 gel was evaluated by constructing 1.6mm thick cell, comprised of two 1mm glass slides with gel trapped in between. Measurements were collected using a spectrophotometer from 300 to 3000 nm. Results can be seen in Figure 4.3.

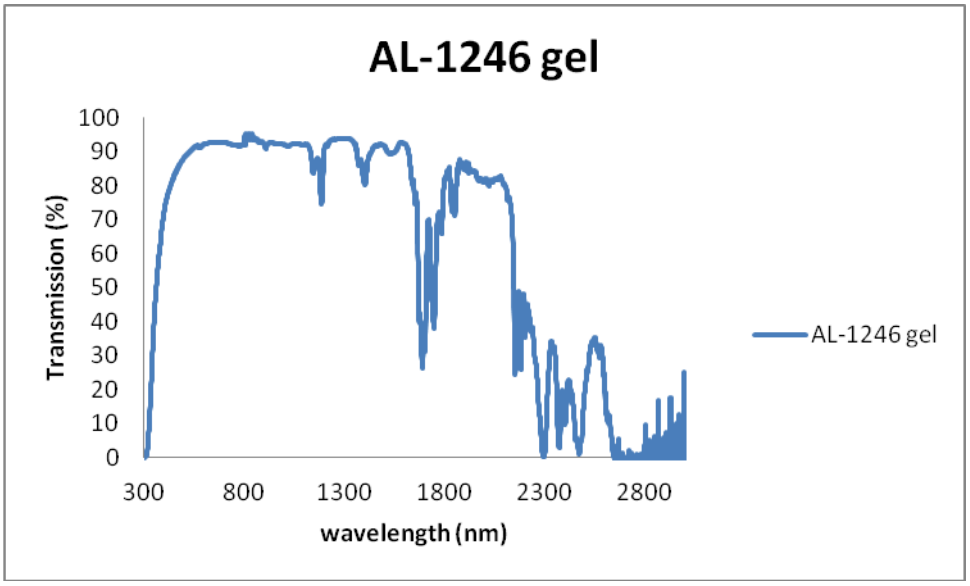

Figure 4.3: Transmission spectrum for GL-1.6mm thick sample.

Comparing transmission of AL-1246 optically clear gel, Sylgard 184 PDMS, water, and LS-6941 optically clear elastomer was accomplished by preparing1.6 mm thick cells with two 1mm thick glass slides. PDMS and elastomer samples were cured per manufacture's requirements. Comparative results can be seen in Figure 4.4 below. AL-1246 transmission measured about 5% less than PDMS. Clearly, PDMS has the best transmission; however, its elongation before failure is 120% and durometer of 44 shore hardness A. These physical properties are not optimum for EL design.

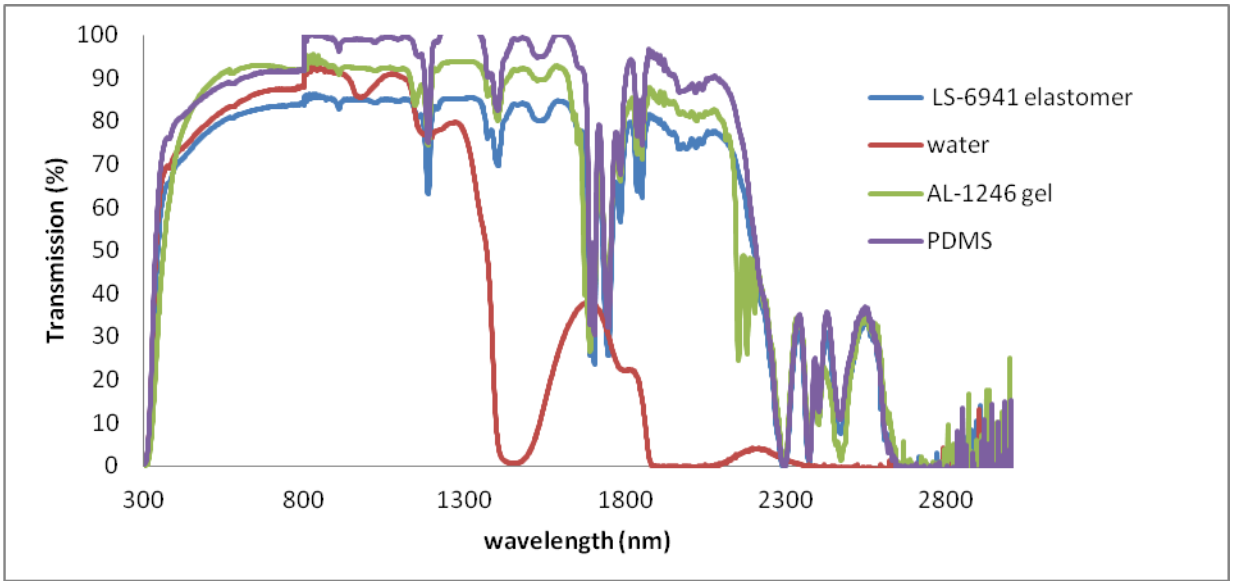

Figure 4.4:Transmission spectrum 1mm thick sample of AL-1246 optically clear gel, Sylgard 184 PDMS, water, and LS-6941 optically clear elastomer.

As with EL, GL was analyzed using a SEM/EDS. The results (Figure 4.5) are very similar to EL; suggesting that the compounds for EL and GL maybe similar, especially when the transmission plots (specifically absorption drops) are compared (see Figure 3.6).

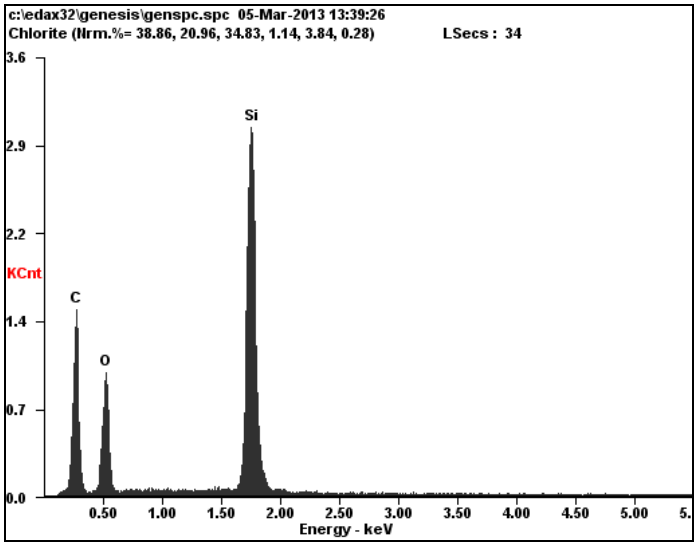

Figure 4.5: SEM/EDS analysis of AL-1246.

Absorption data for AL-1246 is publically available [43] and displayed in Figure 4.6.

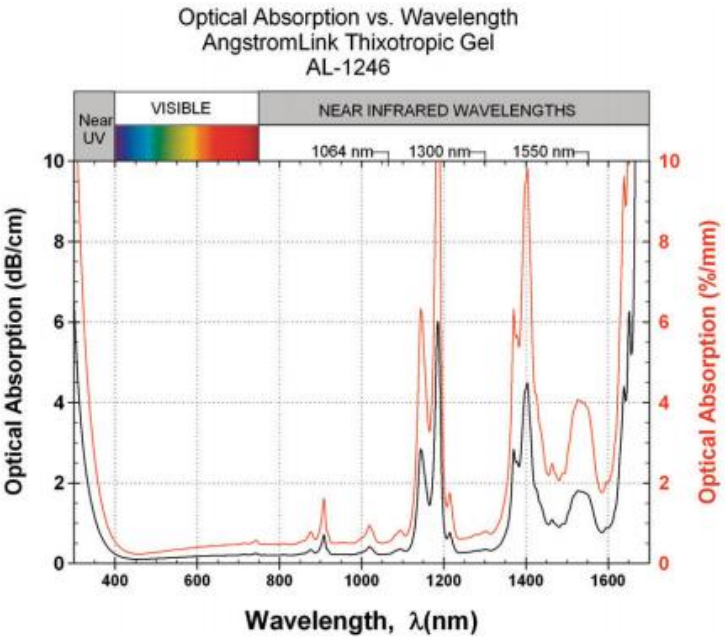

.

Figure 4.6: Absorption spectrum of AL-1246 (permission granted from Fiber Optic Center).

The refractive index of AL-1246 is publically available [43] and shown in Figure 4.7.

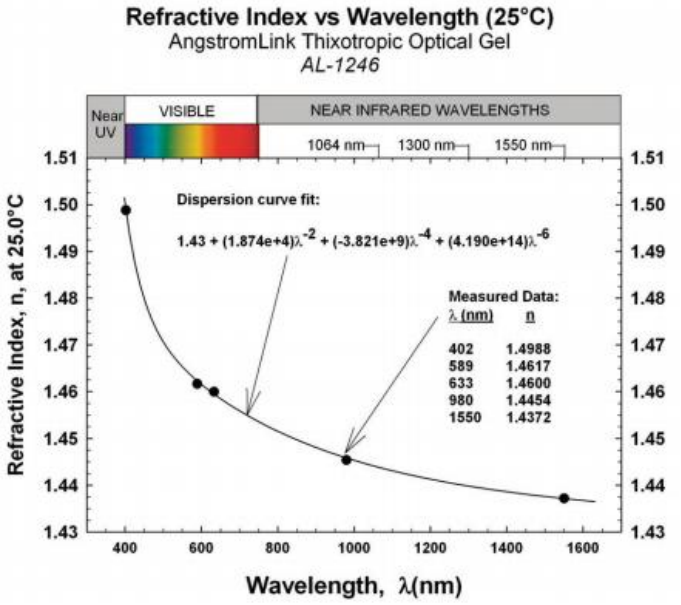

Figure 4.7: Index of refraction curve for AL-1246 (permission granted from Fiber Optic Center).

4.5 Measuring Focal Length

Focal length of the GL lens was approximated by placing the maximum threaded (plano–convex state) EL in front of collimated and expanded He–Ne laser beam (Figure 3.7) and the minimum spot size location was traced (see Figure 3.8). The back focal length (BFL) (and in this case, same as the focal length) was found to be 14 mm. Clear aperture (CA) of GL was 7.9 mm

4.6 Determining Resolution

As in CHAPTER 3, USAF 1951 resolution target (

Figure 4.8) was used to determine the resolution of GL. The exact magnification and resolution setting and capability of the used microscope were not known, so results were approximate. In plano–plano state, Group 3, Element 6 was resolved. This equated to 14.30 lp per mm. As the GL chamber was collapsed and GL took the shape of a plano–convex lens, the

resolution dropped and distortions were introduced. The drop in resolution was due to membrane defects and GL manufacturing complications.

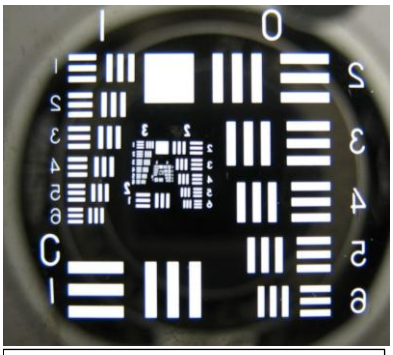

Reference USAF 1951 resolution target

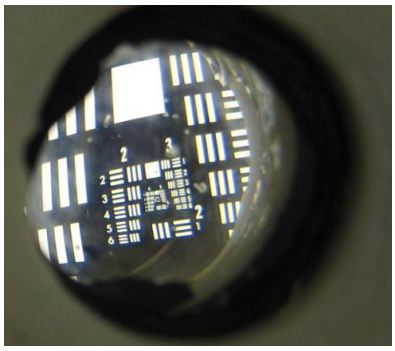

GL in in plano-plano state

Figure 4.8: GL resolution evaluation via a USAF 1951 resolution target.

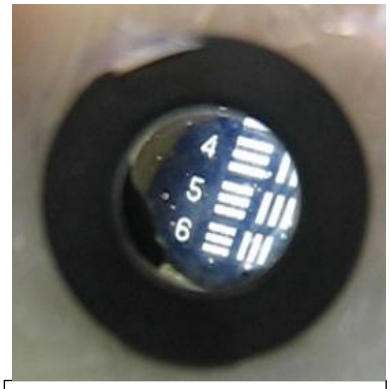

GL in in plano-plano state

GL in in plano-convex state

Figure 4.9: GL in plano-plano and plano-convex states

Comparing the above to a water-filled lens in plano–plano state, 10.10 lp per mm (same as the GL) was resolvable; in plano–convex, 14.3 lp per mm was resolved (Figure 4.10).

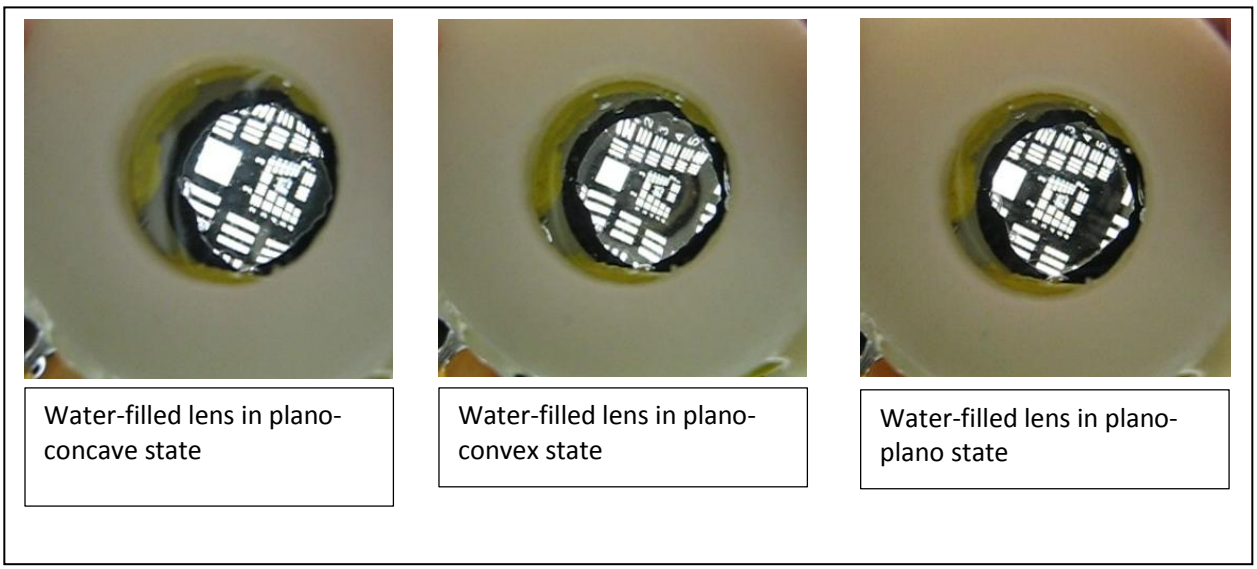

Figure 4.10: A comparison resolution evaluation of GL using water-filled adaptive lens.

4.7 Summary

This chapter describes the demonstration and characterization of an adaptable lens comprised of a collapsible chamber and thixotropic gel AL-1246, which was captured with a PDMS and a glass slide. Thixotropic gel was chosen because of its relative ability to resist deformation under gravitational pull, especially when compared to viscous fluids, and because of its ability to restrict wave (ripple) propagation on the surface due to vibrations.

The mechanical design of focal length manipulation was able to induce both a positive and negative focal length range by collapsing and expanding the collapsible chamber. Almost any adaptive lens design that uses liquid as a substrate, can substitute liquid with optically clear thixotropic gel. This improves lens power by using a higher refractive index gel, when compared

to liquid used, and spectral range can be expanded and/or shifted depending on the liquid and gel replacement.

The spectral range of the evaluated GL spanned from the visible to the NIR region. Resolution was limited by the quality of an elastic membrane, encapsulating thixotropic gel. PDMS membrane was made using a spin-coat method. Further improvements to resolution could have been made by increasing the surface flatness of the PDMS membrane [44] and/or membrane mounting method.

CHAPTER 5. PERFORMANCE IMPROVEMENTS SUGGESTIONS

5.1 Improving Focal Range

As mentioned previously, the focal range of EL can be improved by choosing an optically clear material with a higher index of refraction and higher elongation before failure properties. In addition, molding the lens with a pre-determined radii, as suggested by G. Beadie [2], results in larger variety of focal length ranges.

In addition, EL was made into a lens array system by designing multiple clear apertures on the housing surface that contacts the EL.

5.2 Improving Transmission

An improvement in transmission can be achieved by introducing an AR coating made out of another elastomer. Selection of such elastomer can be made by either procuring or formulating an optically clear elastomer with an index of refraction closely matching to η_c from a well-known formula [45] or finding a close match

$$n_c = \sqrt{n_0 n_s} \tag{11}$$

where η_c is the coating index of refraction, η_o is the medium index of refraction, and η_s is the refractive index of substrate (in this case, the elastomer).

The thickness of the AR coating should be ¼ of the wavelength of interest. For a visible spectrum, the thickness needs to be in the range of 150 nm. This could, perhaps, be achieved by diluting the uncured elastomer and spin coating on top of the substrate of already cured elastomer [46].

5.3 Shifting the Transmittance Spectrum

By manipulating the chemistry of the elastomer, it is perhaps possible to extend or shift the transmittance spectrum into the desirable mid- and far-IR spectrum.

5.4 Summary

Because optically clear thixotropic gel exhibits some liquid and some solid properties, this gel, which makes up the GL, is a promising substitute for some liquid-filled adaptive lenses. This gel could be further formulated for a desired (within some limits) spectral range, while providing a higher index of refraction and physical flexibility.

CHAPTER 6. SUMMARY

Optical and physical attributes of two adaptive lenses were thoroughly evaluated in the research described in this document. Although both had positive and negative attributes, neither surpassed commercially available adaptive lenses in their focal length range or resolution capabilities.

ML-20-35 adaptive lens, made by Optotune, has a focal length range from –40 mm to +40 mm. At 8 mm thickness, ML-20-35 has transmission very similar to EL (at 6 mm in thickness) [47]. Both lenses are proof of concept and can be further refined via manufacturing process improvements.

No vibrational effect is reported for ML-20-35; however, vertical and horizontal orientation effect of lens performance is evaluated and reported to be almost negligible [47].

EL exhibited remarkable stability in any orientation and was able to absorb vibrational waves very well; however, EL is unable to take a concave shape and is limited in optical properties due to physical properties selection. GL is able to shift from concave to convex shape but is not nearly as stable when exposed to vibrations or placed in a vertical orientation.

Further research in material alternatives is necessary to improve spectral range of EL and GL.

LIST OF REFERENCES

1. B. M. Wright, "Improvements in or Relating to Variable Focus Lenses", (1968).

2. G. Beadie, M. L. Sandrock, M. J. Wiggins, R. S. Lepkowicz, J. S. Shirk, M. Ponting, Y. Yang, T. Kazmierczak, A. Hiltner and E. Baer, "Tunable Polymer Lens", Opt. Express **16** (16), 11847-11857, (2008).

3. L. Sz-Yuan, T. Hsi-Wen, C. Wen-Chih and F. Weileun, In *Solid-State Sensors, Actuators and Microsystems Conference, 2007. TRANSDUCERS 2007. International* **2007**, p2147-2150.

4. D.-Y. Zhang, V. Lien, Y. Berdichevsky, J. Choi and Y.-H. Lo, "Fluidic Adaptive Lens with High Focal Length Tunability", Applied physics letters **82** (19), 3171-3172, (2003).

5. H. Ren and S.-T. Wu, "Variable-Focus Liquid Lens", Opt. Express **15** (10), 5931-5936, (2007).

6. D.-Y. Zhang, N. Justis and Y.-H. Lo, "Integrated Fluidic Adaptive Zoom Lens", Optics letters **29** (24), 2855-2857, (2004).

7. A. Mackintosh, A. Kuehne, R. Pethrick, B. Guilhabert, E. Gu, C. Lee, M. Dawson, G. Heliotis and D. Bradley, "Novel Polymer Systems for Deep Uv Microlens Arrays", Journal of Physics D: Applied Physics **41** (9), 094007, (2008).

8. A. Werber and H. Zappe, "Tunable Microfluidic Microlenses", Appl. Opt. **44** (16), 3238-3245, (2005).

9. D.-Y. Zhang, N. Justis, V. Lien, Y. Berdichevsky and Y.-H. Lo, "High-Performance Fluidic Adaptive Lenses", Appl. Opt. **43** (4), 783-787, (2004).

10. H. Oku, K. Hashimoto and M. Ishikawa, "Variable-Focus Lens with 1-Khz Bandwidth", Opt. Express **12** (10), 2138-2149, (2004).

11. C. A. Lopez, C.-C. Lee and A. H. Hirsa, "Electrochemically Activated Adaptive Liquid Lens", Applied Physics Letters **87** (13), 134102-134102-134103, (2005).

12. L. Dong, A. K. Agarwal, D. J. Beebe and H. Jiang, "Adaptive Liquid Microlenses Activated by Stimuli-Responsive Hydrogels", Nature **442** (7102), 551-554, (2006).

13. S. Xu, H. Ren, Y.-J. Lin, M. Moharam, S.-T. Wu and N. Tabiryan, "Adaptive Liquid Lens Actuated by Photo-Polymer", Optics Express **17** (20), 17590-17595, (2009).

14. M. Sandrock, M. Wiggins, J. S. Shirk, H. Tai, A. Ranade, E. Baer and A. Hiltner, "A Widely Tunable Refractive Index in a Nanolayered Photonic Material", Applied Physics Letters **84** (18), 3621-3623, (2004).

15. Y. Zhao, Y. Zhang, R. Lv and Q. Wang, "Novel Optical Devices Based on the Tunable Refractive Index of Magnetic Fluid and Their Characteristics", Journal of Magnetism and Magnetic Materials **323** (23), 2987-2996, (2011).

16. I. J. G. Sparrow and P. G. R. Smith, In *Lasers and Electro-Optics Europe, 2005. CLEO/Europe. 2005 Conference on* **2005**, p491.

17. H. Ren and S. T. Wu, "Introduction to Adaptive Lenses", (Wiley, 2012).

18. X. Zeng and H. Jiang, "Tunable Liquid Microlens Actuated by Infrared Light-Responsive Hydrogel", Applied Physics Letters **93** (15), 151101-151101-151103, (2008).

19. L. Dong and H. Jiang, "Ph-Adaptive Microlenses Using Pinned Liquid-Liquid Interfaces Actuated by Ph-Responsive Hydrogel", Applied physics letters **89** 211120, (2006).

20. B. Hendriks, S. Kuiper, M. Van As, C. Renders and T. Tukker, "Electrowetting-Based Variable-Focus Lens for Miniature Systems", Optical review **12** (3), 255-259, (2005).

21. S. Kuiper and B. H. W. Hendriks, "Variable-Focus Liquid Lens for Miniature Cameras", Applied Physics Letters **85** (7), 1128-1130, (2004).

22. B. Berge and J. Peseux, "Variable Focal Lens Controlled by an External Voltage: An Application of Electrowetting", The European Physical Journal E: Soft Matter and Biological Physics **3** (2), 159-163, (2000).

23. B. Tater, "Baldock, G. R. / Bridgeman, T., the Mathematical Theory of Wave Motion. New York-Chichester-Brisbane-Toronto, John Wiley & Sons and Ellis Hørwood Limited, Chichester 1981. 261 S., £ 19.50. Isbn 0-470-27 113-2", ZAMM - Journal of Applied Mathematics and Mechanics / Zeitschrift für Angewandte Mathematik und Mechanik **62** (7), 350-350, (1982).

24. O. A. Godin and I. M. Fuks, "Transmission of Acoustic-Gravity Waves through Gas–Liquid Interfaces", Journal of Fluid Mechanics **709** (1), 313-340, (2012).

25. O. A. Godin, "Reciprocity and Energy Theorems for Waves in a Compressible Inhomogeneous Moving Fluid", Wave Motion **25** (2), 143-167, (1997).

26. L. M. G. Brekhovskikh, O. A., "Acoustics of Layered Media 2: Point Sources and Bounded Beams", (Springer, 1999).

27. A. d. Bever, WFW-report: 92.006, **1992**.

28. Z. Malacara and M. Servín, "Interferogram Analysis for Optical Testing, Second Edition", (Taylor & Francis, 2010).

29. L. S. Srinath, "Advanced Mechanics of Solids", (McGraw-Hill Education (India) Pvt Limited, 2009).

30. H. H. Rieke and G. V. Chilingarian, "Compaction of Argillaceous Sediments", (Elsevier Science, 1974).

31. M. F. Ashby, H. Shercliff and D. Cebon, "Materials: Engineering, Science, Processing and Design", (Elsevier Science, 2009).

32. R. K. Bansal, "A Textbook of Strength of Materials", (Laxmi Publications Pvt Limited, 2010).

33. e. t. box, In *Elastic Properties and Young Modulus for some Materials* **2013**.

34. Q. Yang, P. Kobrin, C. Seabury, S. Narayanaswamy and W. Christian, "Mechanical Modeling of Fluid-Driven Polymer Lenses", Appl. Opt. **47** (20), 3658-3668, (2008).

35. R. M. A. Azzam and N. M. Bashara, "Ellipsometry and Polarized Light", (North-Holland Pub. Co., 1977).

36. G. Chartier, "Introduction to Optics", (Springer Science+Business Media, Incorporated, 2005).

37. B. S. Naimullah, M. Othman, A. K. Rahman, S. I. Sulaiman, S. Ishak, S. Hitam and S. A. Aljunid, In *Electronic Design, 2008. ICED 2008. International Conference on* **2008**, p1-5.

38. A. A. Vigasin, A. I. Pavlyuchko, Y. Jin and S. Ikawa, "Density Evolution of Absorption Bandshapes in the Water Vapor Oh-Stretching Fundamental and Overtone: Evidence for Molecular Aggregation", Journal of Molecular Structure **742** (1–3), 173-181, (2005).

39. R. Lemus, "Vibrational Excitations in H2o in the Framework of a Local Model", Journal of Molecular Spectroscopy **225** (1), 73-92, (2004).

40. L. Bokobza and O. Rapoport, "Filled Elastomers: Mid- and near-Ir Spectroscopic Determination of Rubber Dimensions in Composite in Unstretched State and under Uniaxial Extension", Journal of Applied Polymer Science **87** (8), 1204-1208, (2003).

41. B. H. Stuart, "Infrared Spectroscopy: Fundamentals and Applications", (Wiley, 2004).

42. S. R. Sandler, W. Karo, J. A. Bonesteel and E. M. Pearce, "Polymer Synthesis and Characterization: A Laboratory Manual", (Elsevier Science, 1998).

43. R. Elgin; Fiber Optic Center.

44. S. E. Sarma and S. Krishnan, On the Manufacture of Very Thin Elastomeric Films by Spin-Coating, Massachusetts Institute of Technology, **2007**.

45. E. Hecht, "Optics", (Pearson Education, 2008).

46. A. L. Thangawng, R. S. Ruoff, M. A. Swartz and M. R. Glucksberg, "An Ultra-Thin Pdms Membrane as a Bio/Micro–Nano Interface: Fabrication and Characterization", Biomedical Microdevices **9** (4), 587-595, (2007).

47. F. Schneider, J. Draheim, R. Kamberger, P. Waibel and U. Wallrabe, "Optical Characterization of Adaptive Fluidic Silicone-Membrane Lenses", Opt. Express **17** (14), 11813-11821, (2009).